Physics Letters B 692 (2010) 327–335

Contents lists available at ScienceDirect

Physics Letters B

www.elsevier.com/locate/physletb

Tevatron Higgs mass bounds: Projecting U(1)′ models to LHC domain

Hale Sert [a,*], Elif Cincioğlu [b], Durmuş A. Demir [a], Levent Solmaz [b]

[a] Department of Physics, İzmir Institute of Technology, TR35430, İzmir, Turkey
[b] Department of Physics, Balıkesir University, TR10145, Balıkesir, Tur

ARTICLE INFO

Article history:
Received 24 March 2010
Received in revised form 2 May 2010
Accepted 5 May 2010
Available online 5 August 2010
Editor: M. Cvetič

Keywords:
Supersymmetric U(1)′ models
Neutral Higgs bosons
Tevatron Higgs measurements

ABSTRACT

We study Higgs boson masses in supersymmetric models with an extra U(1) symmetry to be called U(1)′. Such extra gauge symmetries are urged by the μ problem of the MSSM, and they also arise frequently in low-energy supersymmetric models stemming from GUTs and strings.

We analyze mass of the lightest Higgs boson and various other particle masses and couplings by taking into account the LEP bounds as well as the recent bounds from Tevatron experiments. We find that the μ-problem motivated generic low-energy U(1)′ model yields Higgs masses as large as ~ 200 GeV and violate the Tevatron bounds for certain ranges of parameters. We analyze correlations among various model parameters, and determine excluded regions by both scanning the parameter space and by examining certain likely parameter values. We also make educated projections for LHC measurements in light of the Tevatron restrictions on the parameter space.

We further analyze certain benchmark models stemming from E(6) breaking, and find that they elevate Higgs boson mass into Tevatron's forbidden band when U(1)′ gauge coupling takes larger values than the one corresponding to one-step GUT breaking.

1. Introduction

Minimal supersymmetric model (MSSM) is the most economic extension that can solve the naturalness problem associated with the Higgs sector of the Standard Model (SM) of strong and electroweak interactions [1]. It is an economical description since it is based on the particle spectrum and gauge structure of the SM. Whether it is supersymmetric or not, if the gauge structure is extended to include new factors or embedded in a larger group then there necessarily arise novel particle spectra and phenomena that can be tested via collider experiments or astrophysical observations.

The simplest gauge extension of the MSSM would be to expand its gauge group by an additional Abelian factor – to be hereon called U(1)′ invariance. The most direct motivation for such an extra group factor is the need to solve the μ problem of the MSSM [2]. Indeed, the mass term of the Higgsinos

$$\hat{W}_{MSSM} \ni \mu \hat{H}_u \cdot \hat{H}_d \tag{1}$$

involves a dimensionful parameter μ which is completely unrelated to the soft supersymmetry breaking sector containing the mass parameters in the theory. For consistent electroweak breaking, the soft supersymmetry breaking mass parameters must lie at the electroweak scale, and there is no clue whatsoever why μ should be fixed to this very scale. For naturalizing the μ parameter a viable approach is to associate μ to the vacuum expectation value (VEV) of a new scalar [3]

$$\mu \propto \langle S \rangle \tag{2}$$

where the chiral superfield $\hat{S}$ replaces the bare μ parameter in (1) via

$$\hat{W} \ni h_s \hat{S} \hat{H}_u \cdot \hat{H}_d \tag{3}$$

with h_s being a Yukawa coupling. For the new superpotential not to contain a bare μ term like (1) it is obligatory that the U(1)′ charges of the all superfields sum up to zero by gauge invariance

$$Q_S + Q_{H_u} + Q_{H_d} = 0. \tag{4}$$

Clearly, $Q_S \neq 0$. These conditions guarantee that a bare μ term as in (1) is forbidden completely, and μ parameter is deemed to arise from the VEV of S via (2).

Every single term in the superpotential satisfies U(1)′ gauge invariance conditions like (4). Nevertheless, there are additional non-trivial constraints necessary to make such models anomaly free, especially when the concerning U(1)′ model deviates from the authentic E(6) structures. The anomalies can be cancelled either by introducing family non-universal charges [4] or by importing novel matter species (mimicking those of GUTs such as E(6)) (see the

* Corresponding author.
E-mail address: halesrt@gmail.com (H. Sert).

0370-2693
doi:10.1016/j.physletb.2010.08.007

second reference in [3]). In the present work we shall assume that anomalies are cancelled by additional matter falling outside the reach of LHC experiments.

The μ problem detailed above is not the only motivation for introducing an extra U(1). Indeed, such extra gauge factors, typically more than a single U(1), arise in effective theories stemming from supersymmetric GUTs and strings [5]. In such models, the U(1) charges of fields are fixed by the unified theory. These models are phenomenologically rich and theoretically ubiquitous in superstring theories and GUTs descending from SO(10) and E(6) groups [6]. The E(6) breaking pattern

$$\begin{aligned} \mathrm{E}(6) &\to \mathrm{SO}(10)\otimes \mathrm{U}(1)_\psi \to \mathrm{SU}(5)\otimes \mathrm{U}(1)_\chi \otimes \mathrm{U}(1)_\psi \\ &\to \mathrm{G}_{SM}\otimes \mathrm{U}(1)' \end{aligned} \tag{5}$$

gives rise to the $\mathrm{G}_{SM}\otimes \mathrm{U}(1)'$ model at low energies. Each arrow in this chain corresponds to spontaneous symmetry breakdown at a specific energy scale. Here, by construction,

$$\mathrm{U}(1)' = \cos\theta_{\mathrm{E}(6)}\mathrm{U}(1)_\psi - \sin\theta_{\mathrm{E}(6)}\mathrm{U}(1)_\chi \tag{6}$$

is a light U(1)′ invariance broken near the TeV scale whereas the other orthogonal combination $\mathrm{U}(1)'' = \cos\theta_{\mathrm{E}(6)}\mathrm{U}(1)_\chi + \sin\theta_{\mathrm{E}(6)} \times \mathrm{U}(1)_\psi$ is broken at a much higher scale not accessible to LHC experiments. The angle $\theta_{\mathrm{E}(6)}$ designates the breaking direction in $\mathrm{U}(1)_\chi \otimes \mathrm{U}(1)_\psi$ space and it is a function of the associated gauge couplings and VEVs that realize the symmetry breaking. Many other models can be constructed from the combination of ψ and χ models leading to a solution for μ problem (an exception is the χ model ($\theta_{\mathrm{E}(6)} = -\frac{\pi}{2}$) where the singlet S acquires vanishing U(1)′ charge) [5].

The extra U(1) gives rise to a number of phenomena not found in the MSSM: Its gauge boson Z' and gauge fermion $\tilde{Z}'$ cause anomalies in various MSSM-specific processes [7,8]. Another point as important as these phenomena concerns the Higgs sector: The Higgs sector of such models differ from those of the SM and MSSM [9] not only by the presence of extra Higgs states but also by the modifications in the masses and couplings of the Higgs bosons [10–12] (for phenomenological consequences of an extra singlet on the masses, couplings and decay widths of Higgs bosons the reader can refer to [11]). In fact, the dependencies of the Higgs masses on the model parameters are different than in the MSSM, and the little hierarchy problem of the MSSM seems to be largely softened in such models [13,4].

At the wake of LHC experiments, it is convenient to study the Higgs boson masses in U(1)′ models. Apart from various mass and coupling ranges favored by the models, the existing bounds from the LEP and Tevatron experiments can guide one to more likely regions of the parameter space. The LEP experiments [14] have ended with a clear preference for the lightest Higgs boson mass:

$$m_h > 114.4\ \mathrm{GeV}. \tag{7}$$

The knowledge of the Higgs mass has recently been further supported by the Tevatron results [15] which state that the lightest Higgs boson cannot have a mass in the range

$$159\ \mathrm{GeV} < m_h < 168\ \mathrm{GeV}. \tag{8}$$

It is clear that LEP bound influences the parameter spaces of the SM, MSSM and its extensions like NMSSM and U(1)′ models. The reason is that the LEP range is covered by all these models of electroweak breaking. However, it is obvious that the Tevatron bound has almost no impact on the MSSM parameter space within which m_h cannot exceed ~ 135 GeV. For the same token, however, the Tevatron bounds can be quite effective for extensions of the MSSM whose lightest Higgs bosons can weigh above $2M_W$. This is the case in NMSSM not explored here and in U(1)′ models [10].

In this work we shall analyze U(1)′ models in regard to their Higgs mass predictions and constrained parameter space under the LEP as well as Tevatron bounds by assuming that the Higgs boson searched by DØ and CDF corresponds to that of the U(1)′ models. In course of the analysis, we shall consider the U(1)′ model achieved by low-energy considerations as well as by high-energy considerations (the GUT and stringy U(1)′ models mentioned above). In each case we shall scan the parameter space to determine the bounds on the model parameters by imposing the bounds from direct searches.

The rest of the Letter is organized as follows: In Section 2 below we discuss certain salient features of the U(1)′ models in regard to collider bounds on $M_{Z'}$. Section 3 is devoted to a detailed analysis of the U(1)′ models selected. In Section 4 we conclude.

2. Phenomenological aspects of U(1)′ models

In this section we provide a brief overview of the fundamental constraints on U(1)′ model. First of all, the U(1)′ model is known to generate the neutrino masses in the correct experimental range via Dirac type coupling. The scalar field S responsible for generating the μ parameter also generates the neutrino Dirac masses [16]. Furthermore, the same model offers a viable cold dark matter candidate via the lightest right-handed sneutrino, and accounts for the PAMELA and Fermi LAT results for positron excess for a reasonable set of parameters [17]. Hence, there is no reason for insisting that the neutralino sector offers a CDM candidate. Our focus in this work is on the Higgs sector to which neutrino sector gives no significant contribution.

An important point which concerns the anomalies. A generic U(1)′ model suffers from triangular anomalies and hence gauge coupling non-unification. In the E(6)-motivated models, by construction, all anomalies automatically cancel out when the complete E(6) multiplets are included. For a generic U(1)′, with minimal matter spectrum, cancellation is non-trivial. One possibility is to introduce U(1)′ models with family-dependent charges [4]. Another possibility is that anomalies are cancelled by heavy states (beyond the reach of LHC) weighing near the TeV scale. We shall follow this possibility.

The Higgs sector of the model, as mentioned before, involves the singlet Higgs S and the electroweak doublets H_u and H_d. All of them are charged under U(1)′ gauge group. The Higgs fields expand around the vacuum state as follows

$$\begin{aligned} H_u &= \frac{1}{\sqrt{2}}\begin{pmatrix} \sqrt{2}H_u^+ \\ v_u+\phi_u+i\varphi_u \end{pmatrix}, \qquad H_d = \frac{1}{\sqrt{2}}\begin{pmatrix} v_d+\phi_d+i\varphi_d \\ \sqrt{2}H_d^- \end{pmatrix}, \\ S &= \frac{1}{\sqrt{2}}(v_s+\phi_s+i\varphi_s), \end{aligned} \tag{9}$$

where H_u^+ and H_d^- span the charged sector involving the charged Goldstone eaten up by the $W^\pm$ boson as well as the charged Higgs boson. The remaining ones span the neutral degrees of freedom: $\phi_{u,d,s}$ are scalars and $\varphi_{u,d,s}$ are pseudoscalars. In the vacuum state

$$\frac{v_u}{\sqrt{2}} \equiv \langle H_u^0\rangle, \qquad \frac{v_d}{\sqrt{2}} \equiv \langle H_d^0\rangle, \qquad \frac{v_s}{\sqrt{2}} \equiv \langle S\rangle \tag{10}$$

the $W^\pm$, Z and Z' bosons all acquire masses. However, the neutral gauge bosons Z and Z' exhibit non-trivial mixing [18,3]. The two eigenvalues of this mixing matrix [18] give the masses of the physical massive vector bosons (M_{Z_1}, M_{Z_2}) where M_{Z_1} must agree with the experimental bounds on the Z boson mass in the MSSM (or SM). The mixing angle $\alpha_{Z-Z'}$ [18] must be a few 10^{-3} for precision measurements at LEP experiments to be respected. This puts

a bound on the Z_2 boson mass. In particular, in generic E(6) models m_{Z_2} must weigh nearly a TeV or more according to the Tevatron measurements [19,20].

Due to the soft breaking of supersymmetry, the Higgs boson masses shift in proportion to particle–sparticle mass splitting under quantum corrections. Though all particles which couple to the Higgs fields S, H_u and H_d contribute to the Higgs boson masses, the largest correction comes from the top quark and its superpartner scalar top quark (and to a lesser extent from the bottom quark multiplet). Including top and bottom quark superfields, the superpotential takes the form

$$\hat{W} \ni h_s \hat{S} \hat{H}_u \cdot \hat{H}_d + h_t \hat{Q} \cdot \hat{H}_u \hat{t}^c_R + h_b \hat{Q} \cdot \hat{H}_d \hat{b}^c_R \tag{11}$$

where h_t and h_b are top and bottom Yukawa couplings. Clearly $\hat{Q}^T = (\hat{t}_L, \hat{b}_L)$. This superpotential encodes the dominant couplings of the Higgs fields which determine the F-term contributions.

Effective potential proves to be an efficient method for computing the radiative corrections to Higgs potential. In fact, the radiatively corrected potential reads as

$$V_{total}(H) = V_{tree}(H) + \Delta V(H) \tag{12}$$

where the tree level potential is composed of F-term, D-term and soft-breaking pieces

$$V_{tree} = V_F + V_D + V_{soft} \tag{13}$$

with

$$V_F = |h_s|^2 \big[|H_u \cdot H_d|^2 + |S|^2 \big(|H_u|^2 + |H_d|^2 \big) \big], \tag{14}$$

$$V_D = \frac{G^2}{8} \big(|H_u|^2 - |H_d|^2 \big) + \frac{g_2^2}{2} \big(|H_u|^2 |H_d|^2 - |H_u \cdot H_d|^2 \big) + \frac{g_Y'^2}{2} \big(Q_{H_u} |H_u|^2 + Q_{H_d} |H_d|^2 + Q_S |S|^2 \big)^2, \tag{15}$$

$$V_{soft} = m_{H_u}^2 |H_u|^2 + m_{H_d}^2 |H_d|^2 + m_s^2 |S|^2 + (h_s A_s S H_u \cdot H_d + \text{h.c.}). \tag{16}$$

The contributions of the quantum fluctuations in (12) read as

$$\Delta V = \frac{1}{64\pi^2} \operatorname{Str} \left[\mathcal{M}^4 \left(\ln \frac{\mathcal{M}^2}{\Lambda^2} - \frac{3}{2} \right) \right] \tag{17}$$

where $\operatorname{Str} \equiv \sum_J (-1)^{2J} (2J+1) \operatorname{Tr}$ is the usual supertrace which generates a factor of 6 for squarks and -12 for quarks. Λ is the renormalization scale and $\mathcal{M}$ is the field-dependent mass matrix of quarks and squarks (we take $\Lambda = m_t + m_{Z_2}/2$). The dominant contribution comes from top quark (and bottom quark, to a lesser extent) multiplet. The requisite top and bottom quark field-dependent masses read as $m_t^2(H) = h_t^2 |H_u^0|^2$, $m_b^2(H) = h_b^2 |H_d^0|^2$. The mass-squareds of their superpartners follow from

$$m_{\tilde{f}}^2 = \begin{pmatrix} M_{\tilde{f}LL}^2 & M_{\tilde{f}LR}^2 \\ M_{\tilde{f}RL}^2 & M_{\tilde{f}RR}^2 \end{pmatrix} \tag{18}$$

where $f = t$ or b. For instance, the entries of the stop mass-squared matrix read to be

$$\begin{aligned} M_{\tilde{t}LL}^2 &= m_{\tilde{Q}}^2 + m_t^2 - \frac{1}{12} \big(3g_2^2 - g_Y^2 \big) \big(|H_u^0|^2 - |H_d^0|^2 \big) + g_Y'^2 Q_Q \big(Q_{H_u} |H_u|^2 + Q_{H_d} |H_d|^2 + Q_S |S|^2 \big), \\ M_{\tilde{t}RR}^2 &= m_{\tilde{t}_R}^2 + m_t^2 - \frac{1}{3} g_Y^2 \big(|H_u^0|^2 - |H_d^0|^2 \big) + g_Y'^2 Q_U \big(Q_{H_u} |H_u|^2 + Q_{H_d} |H_d|^2 + Q_S |S|^2 \big), \\ M_{\tilde{t}LR}^2 &= M_{\tilde{t}RL}^2 = h_t \big(A_t H_u^0 - h_s S H_d^0 \big). \end{aligned} \tag{19}$$

Insertion of the top and bottom mass matrices into (17) generates the full one-loop effective potential. Radiatively corrected Higgs masses and mixings are computed from the effective potential [10].

3. Analysis

In this section we shall perform a numerical analysis of Higgs boson masses in order to determine the allowed regions under the LEP and Tevatron bounds. Our results, with a sufficiently wide range for each parameter, can shed light on the relevant regions of the parameter space to be explored by the experiments at CERN. In the following we will first discuss the parameter space to be employed, and then we shall provide a set of figures each probing certain parameter ranges in the U(1)′ models considered.

3.1. Parameters

In course of the analysis, we shall partly scan the parameter space and partly analyze certain parameter regions which best exhibit the bounds from the Higgs mass measurements. We first list down various parameter values to be used in the scan.

3.1.1. U(1)′ gauge coupling

The U(1)′ models we consider are inherently *unconstrained* in that, irrespective of their low-energy or high-energy origin, we let U(1)′ gauge coupling g_Y' to vary in a reasonable range in units of the hypercharge gauge coupling. We thus call all the models we investigate as 'Unconstrained U(1)′ models', or, UU(1)′ models, in short.

We shall be dealing with four different UU(1)′ models:

- UU(1)′ from E(6) supersymmetric GUT: the η, N and ψ models.
- UU(1)′ from low-energy (solution of the μ problem): this is the low-energy model obtained by taking $Q_{H_u} = Q_{H_d} = Q_Q = -1$ and hence $Q_U = Q_D = Q_S = 2$, and we shall be calling this model the X model.

The charge assignments of E(6)-based models can be found in [18]. For them we use the same symbols but mutate them by giving up the typically-assumed value $g_Y' = \sqrt{\frac{5}{3}(g_2^2 + g_Y^2)} \sin\theta_W$ (obtained by one-step GUT breaking), and changing it in the range g_Y to $2g_Y$. The motivation behind this mutation of the E(6)-based U(1)′ groups is that one-step GUT breaking is too unrealistic to follow; the GUT group is broken at various steps as indicated in (5). Nevertheless, large values of g_Y' may be inadmissibly large for perturbative dynamics, and we shall note this feature while interpreting the figures. Despite this, however, by varying the g_Y' we will treat E(6)-based models as some kind of specific UU′ models in which we can probe the impact of different g_Y' values on the lightest Higgs mass.

Unlike the E(6)-based models, we adopt the value of g_Y' from one-step GUT breaking in analyzing the X model. In X model, by the need to cancel the anomalies, we assume that there exist an unspecified sector of fairly light chiral fields, and normalization of the charge and other issues depend on that sector [3]. Our analysis will be indicative of a generic U(1)′ model stemming from mainly the need to evade the naturalness problems associated with the μ problem of the MSSM.

3.1.2. The gauge and Yukawa couplings

In U(1)′ models, at the tree level one can write $m_h^2 \lesssim a_i + b_i h_s^2$ where a_i, b_i are some constants to be determined from

the given value of $\tan\beta$, charge assignments as well as the soft supersymmetry-breaking sector. Hence, for sufficiently large b_i/a_i ratios, one can expect $m_h \propto h_s$. At one-loop level, it is interesting to probe if such a relation also exists for the gauge coupling, Yukawa coupling and other important model parameters. We will be dealing with this issue numerically, by changing the value of g'_Y as stated above.

3.1.3. The Z–Z' mixing

We shall always require the Z–Z' mixing to obey the bound $|\alpha_{Z-Z'}| < 10^{-3}$ for consistency with current measurements [21]. The collider analyses [20] constrain m_{Z_2} to be nearly a TeV or higher with the assumption that Z_2 boson decays exclusively into the SM fermions. However, inclusion of decay channels into superpartners increases the Z_2 width, and hence, decreases the m_{Z_2} lower bound by a couple of 100 GeVs [18]. But, for simplicity and definiteness, we take $m_{Z_2} \geqslant 1$ TeV as a nominal value.

3.1.4. Ratio of the Higgs VEVs $\tan\beta$

We fix $\tan\beta$ from the knowledge of $\alpha_{Z-Z'}$ [10]: $\tan^2\beta = F_d/F_u$ where

$$F_{u,(d)} = \left(2g'_Y/G\right)Q_{H_{u,(d)}} \pm \alpha_{Z-Z'}\left(-1+\left(2g'_Y/G\right)^2\left(Q^2_{H_{u,(d)}} + Q^2_S\left(v_s^2/v^2\right)\right)\right). \quad (20)$$

Using this expression we find that $\tan\beta$ stays around 1 (this is true as far as v_s is not very large), and thus, we scan $\tan\beta$ values from 0.5 to 5 in E(6)-based models, and in the X model. The post-LEP analyses of the MSSM disfavors $\tan\beta \sim 1$ yet in U(1)′ models as well as in NMSSM there is no such conclusive result. One can in fact, consider $\tan\beta$ values significantly smaller than unity, as a concrete example η model favors $\tan\beta = 0.5$.

3.1.5. The Higgsino Yukawa coupling

Our analysis respects $h_s = 1/\sqrt{2}$ in our X model; this value is suggested by the RGE analysis of [3]. However, not only for our X model but also for our mutated E(6) models we allow h_s to vary from 0.1 to 0.8 for determining its impact on the Higgs boson masses. The Higgsino Yukawa coupling h_s determines the effective μ parameter in units of the singlet VEV v_s.

3.1.6. The squark soft mass-squareds

We scan each of $m_{\tilde{Q}}, m_{\tilde{t}_R}$ and $m_{\tilde{b}_R}$ in $[0.1, 1]$ TeV range. Following the PDG values [22], we require light stop and sbottom to weigh appropriately: $m_{\tilde{t}_1} > 180$ GeV and $m_{\tilde{b}_1} > 240$ GeV. These bounds follow from direct searches at the Tevatron and other colliders.

3.1.7. Singlet VEV v_s

We scan v_s in $[1, 2]$ TeV range so that m_{Z_2} can be larger than 1 TeV. In doing this we set $\mu_{eff} < 1$ TeV as the upper limit of this parameter. Larger values of μ_{eff} are more fine-tuned in such models than the MSSM [11]. Such keen values of v_s and μ_{eff} turn out to be necessary for keeping the mentioned models at the low-energy region and also for satisfying the aforementioned constraints.

3.1.8. Trilinear couplings

In the general scan we vary each of A_t, A_b, A_s in $[-1, 1]$ TeV range, independently. This is followed by a specific scan regarding Tevatron bounds where the trilinears and soft masses of the scalar quarks are assigned to share some common values. We do this for all of the models we are considering.

These parameter regions will be employed in scanning the parameter space for determining the allowed domains. In addition to and agreement with these, we shall select out certain parameter values to illustrate how strong or weak the bounds from Higgs mass measurements can be. The results are displayed in a set of figures in the following subsection.

3.2. Scan of the parameter space

In this subsection we present our scan results for various model parameters in light of the Tevatron and LEP bounds on the lightest Higgs mass. We start the analysis with a general scan using the inputs mentioned in the previous subsection. This will allow us to perform a specific search concentrated around the Tevatron exclusion limits. In both of the scans we will present the results for X model first, which is followed by the E(6)-based models η, N and ψ models.

Related with the general scan we present Fig. 1 wherein h_s, g'_Y and μ_{eff} are variables on the surface (the only exception is X model for which g'_Y is taken at its GUT normalized value). The remaining variables, whose ranges were mentioned in the previous section, vary in the background. In Fig. 1, shown are the variations of the lightest Higgs boson mass against the gauge coupling g'_Y (left panels), Higgsino Yukawa coupling h_s (middle panels), and the effective μ parameter μ_{eff} (right panels).

As are seen from the left panels of Fig. 1, increase in the g'_Y gives rise to higher upper bounds on m_h for E(6)-based models. The same behavior, though not shown explicitly, occurs in the X model (which already yields m_h values as high as 195 GeV). Excepting the η model, the E(6)-based models are seen to accommodate Higgs boson masses larger than the Tevatron upper bound when g'_Y rises to extreme values above ~ 0.8. Needless to say, the regions with grey dots are followed by regions with grey crosses (the forbidden region), as expected from the dependence of the Higgs boson mass on g'_Y. The η model does not touch even the Tevatron lower bound of the excluded region for the parameter values considered.

Depicted in the middle panels of Fig. 1 is the variation of the Higgs boson mass with the Higgsino Yukawa coupling for the models considered. Clearly, h_s parameter is more determinative than g'_Y in that m_h tends to stay in a strip of values for the entire range of h_s. Indeed, upper bound on m_h (and its lower bound, to a lesser extent) varies linearly with h_s for X, N and ψ models. This is also true for the η model at least up to $h_s \sim 0.65$. In general, Tevatron bounds divide h_s values into two disjoint regions separated by the forbidden region yielding m_h values excluded by the Tevatron results. One keeps in mind that, in this and following figures, the η model serves to illustrate E(6)-based models yielding a genuine light Higgs boson: The Higgs boson stays light for the entire range of parameter values considered. At least for the X model, one can write

$$159 \gtrsim m_h \gtrsim 114.4 \quad \Rightarrow \quad h_s \in [0.3, 0.7] \quad \text{and}$$
$$m_h \gtrsim 168 \quad \Rightarrow \quad h_s \in [0.6, 0.8] \quad (21)$$

from the distribution of the allowed regions (top middle panel). More precisely, the Higgsino Yukawa coupling largely determines the ranges of the Higgs mass in that while m_h barely saturates the lower edge of the Tevatron exclusion band for $h_s < 0.52$, it takes values above the Tevatron upper edge for $h_s > 0.58$. In other words, Tevatron bound divides h_s ranges into two regions in relation with m_h values: The h_s values for low m_h ($114.4\ \text{GeV} \leqslant m_h \leqslant 158$ GeV) and those for high m_h ($m_h > 168$ GeV). This distinction is valid for all the variables we are analyzing.

The variation of the Higgs boson mass with the effective μ parameter is shown in the right-panels for Fig. 1, for each model. It is clear that $\mu_{eff} \gtrsim 300$ GeV for the LEP bound to be respected.

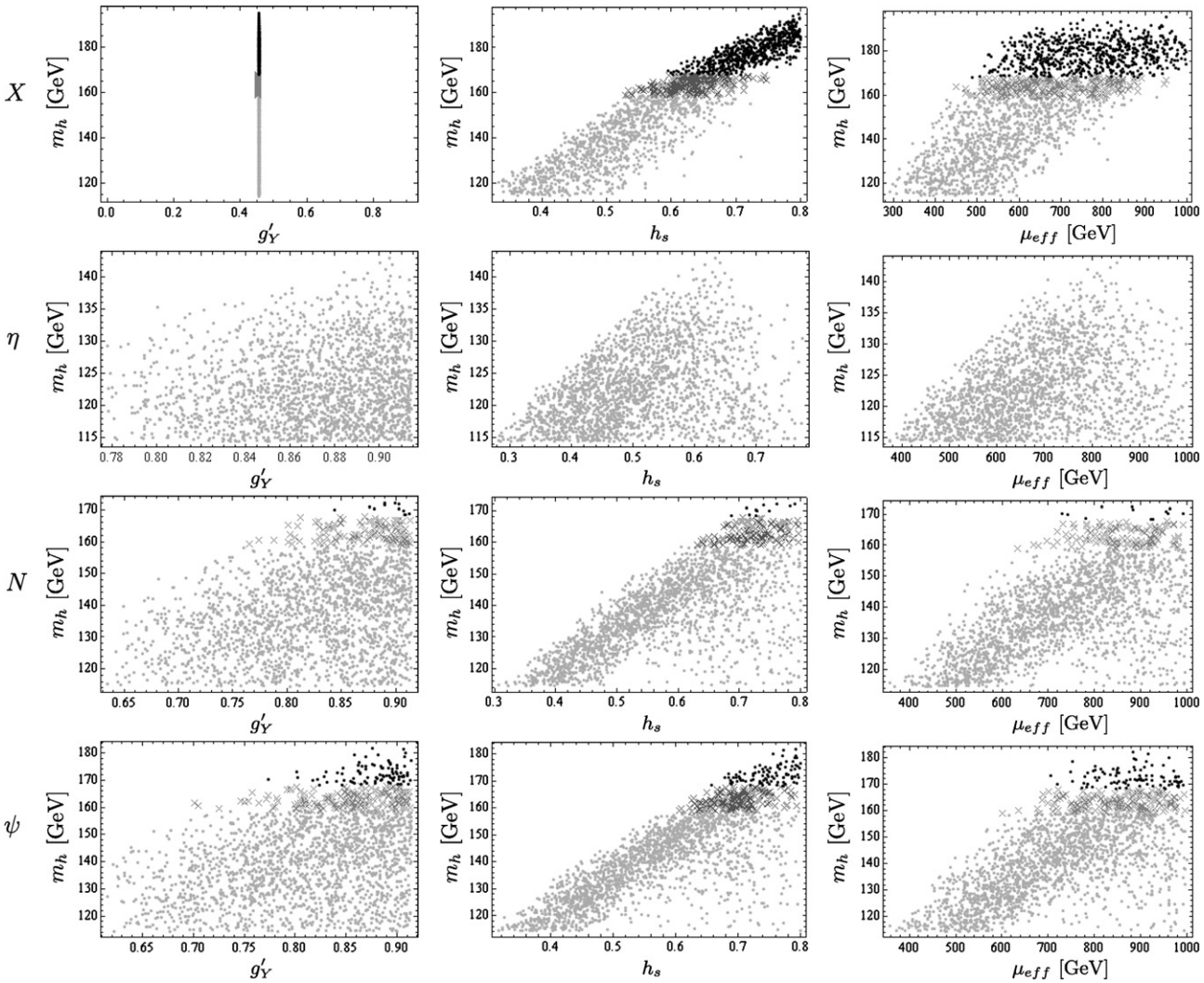

Fig. 1. The plots for the X, η, N and ψ models (from top to bottom). The mass of the lightest Higgs boson against the gauge coupling g'_Y (left panels), Higgsino Yukawa coupling h_s (middle panels), and effective μ parameter (right panels). The shading convention is such that the points giving $m_h > 168$ GeV are shown by black dots, those yielding 114.4 GeV $\leqslant m_h \leqslant$ 159 GeV by grey dots, and those yielding 159 GeV $\leqslant m_h \leqslant$ 168 GeV by grey crosses.

On the other hand, one needs $\mu_{eff} \gtrsim 500$ GeV for m_h to touch the lower limit of the Tevatron exclusion band in the X model. Similar conclusions hold also for the mutated E(6) models: $\mu_{eff} \gtrsim 700$ GeV for ψ and N models (while the forbidden Tevatron territory is never reached in the η model). The η model is bounded by LEP data only (at least within the input values assumed for which we considered $v_s \leqslant 2$ TeV).

From the scans above we conclude that:

- All models are constrained by the LEP bound, that is, each of them predict Higgs masses below 114.4 GeV for certain ranges of parameters.
- The X model, a genuine low-energy realization of UU(1)′ models based solely on the solution of the μ problem, yields large m_h values, and thus, violated the Tevatron forbidden band low values of g'_Y, h_s and μ_{eff} compared to the mutated E(6)-based models. The latter require typically large values of g'_Y, h_s and μ_{eff} for yielding m_h values falling within the Tevatron territory (meanwhile, this can happen only if $g'_Y \gtrsim 0.77$ in N model and $g'_Y \gtrsim 0.7$ in ψ model with a Yukawa coupling saturating $h_s \gtrsim 0.62$). In fact, the η model does not even approach to the 159 GeV border so that it does not feel Tevatron bounds at all. There is left only a small parameter space wherein m_h exceeds 159 GeV for ψ and N models. One can safely say that for 'small' g'_Y and h_s the E(6)-based models predict m_h to be low, significantly below 159 GeV. In other words, Tevatron bounds shows tendency to rule out non-perturbative behavior of E(6)-based models.
- One notices that heavy Higgs limit typically require large μ_{eff} (close to TeV domain) and thus one expects Higgsinos to be significantly heavy in such regions. The LSP is to be dominated by the gauginos, mainly. In such regions, one expects the physical neutralino corresponding to $\tilde{Z}'$ to be also heavy due to the fact that $\tilde{Z}'$ mixes with $\tilde{S}$ by a term proportional to $h_s v_s$ [7]. Therefore, the light neutralinos are to be dominantly determined by the MSSM gauginos.

Using the grand picture reached above, we now perform a point-wise search aiming to cover critical points wherein Tevatron exclusion is manifest. We project implications of these exclusions to scalar fermions and other neutral Higgs bosons. But, for doing this we first fix certain variables, and by doing so, we get rid of overlapping regions (seen in surface parameters while others running in the background).

From Fig. 1, we find it sufficient to consider values around $h_s \sim 0.7$ and $g'_Y \sim 2g_Y$. More precisely, we consider Higgsino Yukawa

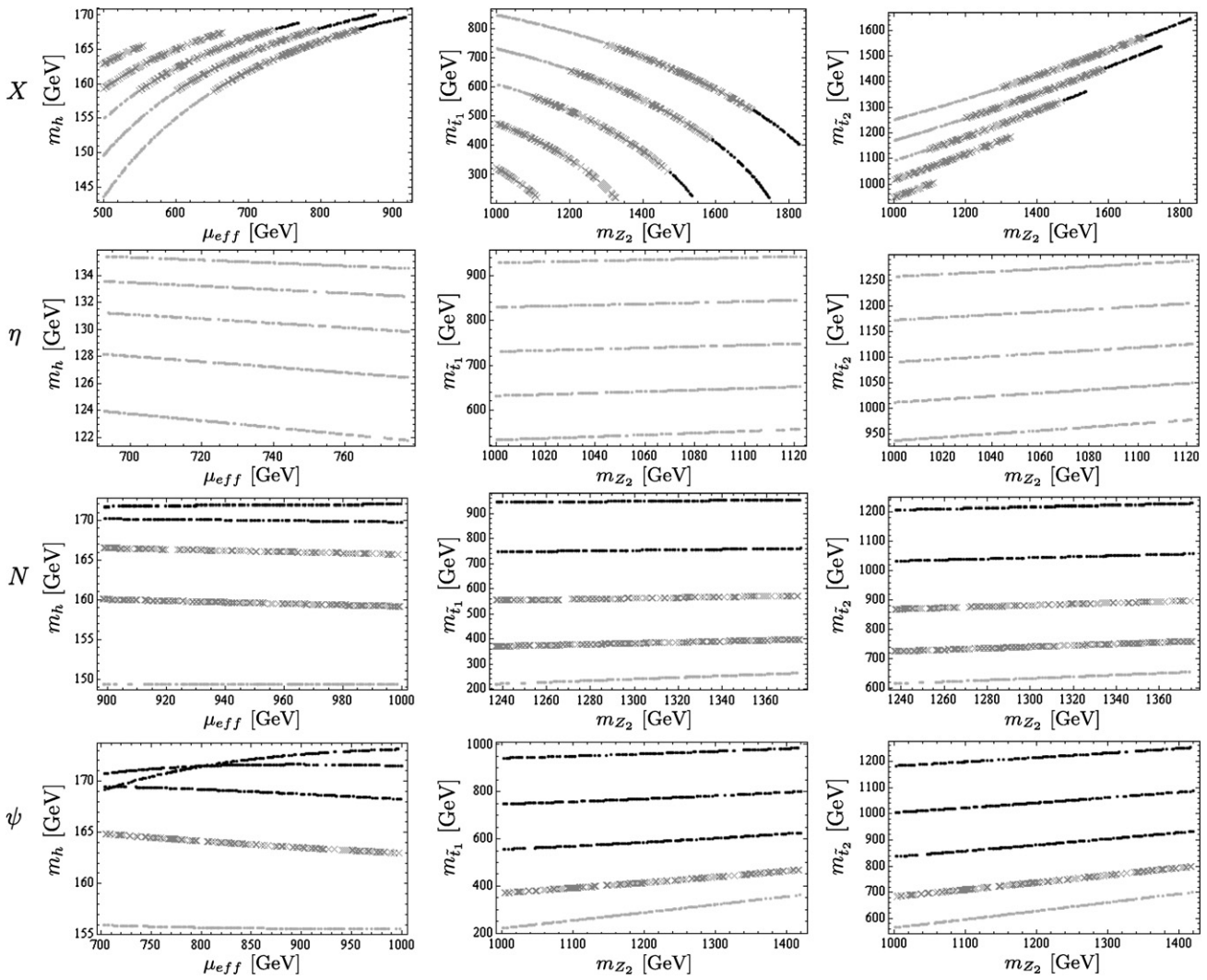

Fig. 2. The mass of the lightest Higgs boson against the effective μ parameter (left panels), the mass of the light scalar top $m_{\tilde{t}_1}$ against the mass of the Z_2 boson (middle panels), and the mass of the heavy scalar top $m_{\tilde{t}_2}$ against the mass of the Z_2 boson (right panels) in X, η, N and ψ models (top to bottom). Our shading convention is the same as in Fig. 1. The inputs are selected as: $m_{common} = m_{\tilde{Q}} = m_{\tilde{t}_R} = m_{\tilde{b}_R} = -A_t = -A_b = -A_s = 0.2$ to 1 TeV with increments 200 GeV in N and ψ models. In X and η models we scan m_{common} from 0.5 to 1 TeV with increments 100 GeV. These inputs are also used in the following figure. In any panel of the figures we observe a hierarchy such that largest m_{common} value corresponds to the largest m_h value (topmost data lines) which is fixed at 1 TeV.

couplings as $h_s = 0.65, 0.5, 0.7$ and 0.7 for X, η, N and ψ models, respectively. We set $g'_Y = 1.9 g_Y$ for all three mutated E(6) models, while we keep it as in Fig. 1 for the X model.

In Fig. 2, depicted are variations of the m_h and scalar top quark masses ($m_{\tilde{t}_1}$ and $m_{\tilde{t}_2}$) with μ_{eff} and M_{Z_2}. This is the targeted search. Now, as can be seen from the left panels of Fig. 2, the effective μ parameter should satisfy $\mu_{eff} > 500$ GeV in X model, while others demanding higher values. This is due to already fixed h_s parameter value. In this figure, the impact of Tevatron exclusions is seen clearly (gray crosses) on scalar fermions (middle and right panels of X, N and ψ models), too. It is interesting to check model dependent issues for this sector because the scalar fermions shall be important for discriminating among the supersymmetric models (even among the U(1)′ models) at the LHC and ILC. The goal of Fig. 2 is to serve this aim, in which scalar quark masses are plotted against varying Z_2 boson mass (middle and right panels). The correlation between sfermion masses and M_{Z_2} comes mainly from the U(1)′ D-term contributions (proportional to $g'^2_{Y'} v_s^2$) to the LL and RR entries of the sfermion mass-squared matrices. There are also F-term contributions proportional to $h_s v_s$ to LR entries but their effects are much smaller compared to those in the LL and RR entries (see Eq. (19) for details). This is an important effect not found in the minimal model: variation of sfermion masses with μ probes only the LR entry in the MSSM. It is in such extensions of the MSSM that one finds explicit dependence on μ_{eff} in not only the LR entries but also in LL and RR entries; effects of μ_{eff} are more widespread than in the minimal model where μ is regarded as some external parameter determined from the electroweak breaking condition.

From Fig. 2 one concludes that variations of m_h and $m_{\tilde{t}_{1,2}}$ are much more violent in X model than in the E(6)-based models. In the X model changes in M_{Z_2} and μ_{eff} influence Higgs and stop masses violently so that allowed and forbidden regions are seen rather clearly. In E(6)-based models what we have nearly constant strips, and thus, m_h and $m_{\tilde{t}_{1,2}}$ remain essentially unchanged with μ_{eff} and M_{Z_2}. Moreover, in mutated E(6) models the forbidden regions and allowed regions fall into distinct strips, signalling thus the aforementioned near constancy of the Higgs and stop masses. From Fig. 2 it is possible to read out certain likely ranges for stop and Higgs boson masses, which will be key observables in collider experiments like LHC and ILC. Indeed, in X model one deduces that

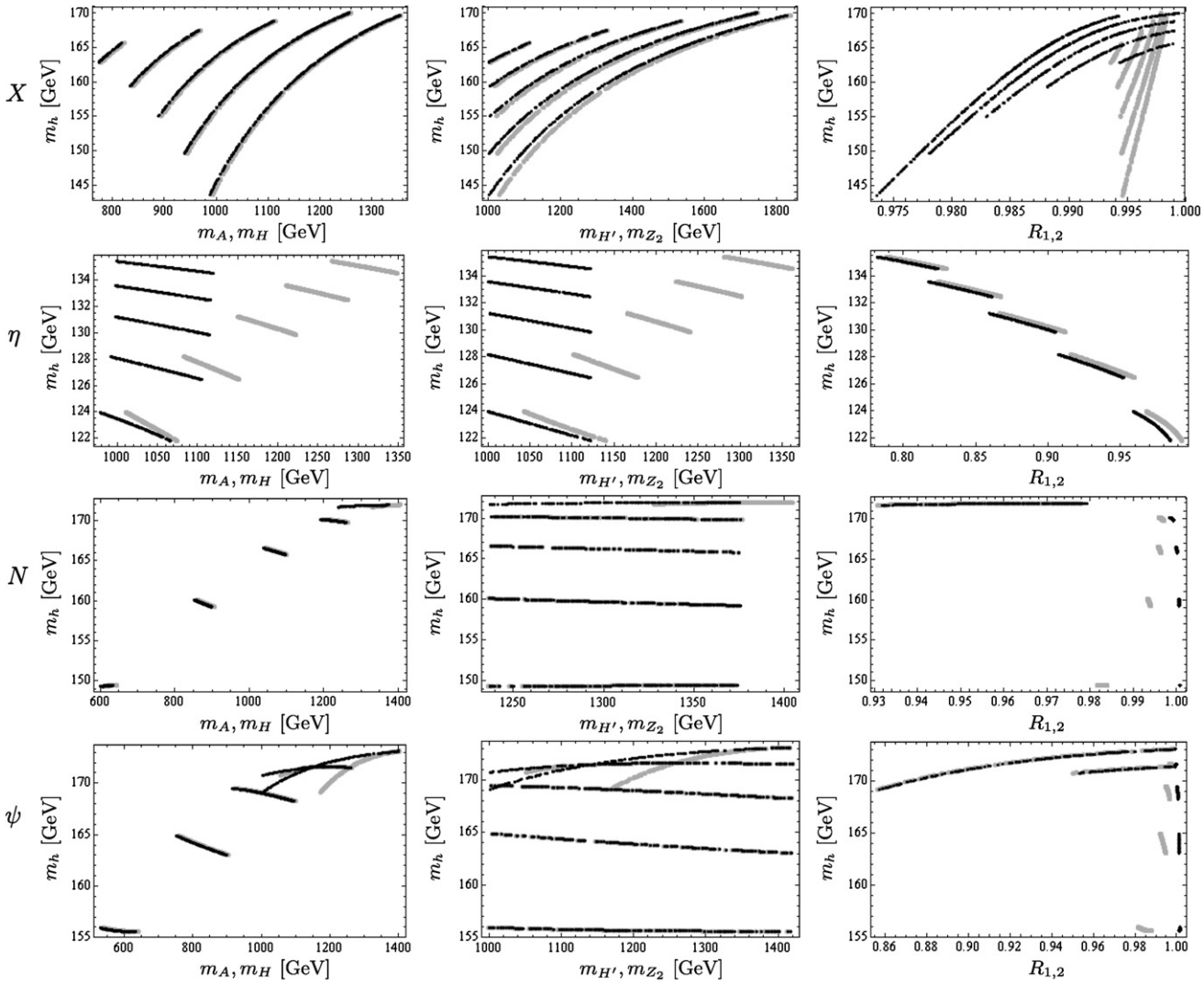

Fig. 3. Variations of the lightest Higgs boson mass m_h with those of the heavy CP-even Higgs scalars H, H' and of the CP-odd scalar A. Also given is the dependence of m_h on the Z_2 boson mass. In the decoupling region, $m_H \sim m_A$ and $m'_H \sim m_{Z_2}$. The notation is such that m_A and $m_{H'}$ are denoted by grey dots, m_H and m_{Z_2} by black dots. As a measure of the approach to the decoupling region, we explore, in the right panels, the quantities R_1 (gray dots) and R_2 (black dots). The input parameters are taken as in Fig. 2.

- Higgs in low-mass region $\Rightarrow m_{\tilde{t}_1} \in [600, 800]$ GeV and $m_{Z_2} \in [1.0, 1.3]$ TeV,
- Higgs in high-mass region $\Rightarrow m_{\tilde{t}_1} \in [200, 550]$ GeV and $m_{Z_2} \in [1.5, 1.8]$ TeV.

Therefore, in principle, taking the X model as the underlying setup, one can determine if Higgs is in the low- or high-mass domains by a measurement of the scalar top quark masses. For instance, if collider searches exclude low-mass light stops up to ~ 600 GeV then one immediately concludes that the Higgs boson should be light, i.e. below $2M_W$.

Contrary to model X, E(6)-based models N and ψ allow the Z' mass to be more confined, i.e. the mass of the Z_2 boson is in $\sim [1, 1.4]$ TeV range within these two models. Furthermore, these two models can rule out $m_{\tilde{t}_1}$ around $\sim [300, 500]$ GeV (one keeps in mind, however, that in these models low (high) stop mass values are related with low (high) m_h values, in contradiction with the X model). Besides this, all three of X, N and ψ models exploration of *high-mass* region demands larger values for $m_{\tilde{t}_2}$. One notices that largest (smallest) splitting between $m_{\tilde{t}_2}$ and $m_{\tilde{t}_1}$ is observed in X (ψ) model. As an extension of the MSSM, the present model predicts 3 CP-even Higgs bosons: h, H and H'. There is no analogue of H' in the MSSM. The mode predicts one single pseudoscalar Higgs boson A as in the MSSM. In the decoupling regime i.e. when heavier Higgs bosons decouple from h one expects the mass hierarchy $m_{H'} \sim m_{Z_2} \gg m_H \sim m_A \gg m_h$. It is thus convenient to analyze the model in regard to its Higgs mass spectra to determine in what regime the model is working. To this end, we depict variations of m_h with m_H, m'_H and m_{Z_2} in Fig. 3. For quantifying the analysis we define the ratios $R_1 \equiv \frac{m_H}{m_A}$, $R_2 \equiv \frac{m_{Z_2}}{m_{H'}}$ which are, respectively, shown by gray and black dots in Fig. 3.

In Fig. 3, shown in the leftmost column are variations of m_h with m_H (black dots) and with m_A (grey dots). It is clear that, the X and N models are well inside the decoupling regime for the parameter ranges considered. On the other hand, the ψ and η models, especially the η model, are far from their decoupling regime. In this regime, the lightest Higgs can weigh well above its lower bound. One notices that, A and H bosons exhibit no sign of degeneracy in the η model.

The variations of m_h with m'_H and m_{Z_2} are shown in the middle column of Fig. 3. One observes that grand behavior is similar to those in the first column. One, however, makes the distinction that

m_h depends violently on m'_H and m_{Z_2} in X and η models while it stays almost completely independent for ψ and N models.

All the properties summarized above are quantified in the third column wherein m_h is plotted against R_1 and R_2. The degree to which $R_{1,2}$ measure close to unity give a quantitative measure of how close the parameter values are to the decoupling regime. One notices that they differ significantly from unity in η and ψ models. In summary, m_A/m_H ratio drops to ~ 0.8 in η model. This is also true for $m_{Z_2}/m_{H'}$. It is interesting to observe that R_1 and R_2 behave very similar in most of the parameter space. This figure depicts the heavy model dependency of neutral Higgs masses.

Experiments at the LHC and ILC will be able to measure all these Higgs boson masses, couplings and decay modes [11]. Clearly, η and ψ (especially ψ) model yield lightest of H, A among all the models considered. In course of collider searches, these two models will be differentiated from the others by their relatively light heavy-Higgs sector.

4. Conclusion

In this work we have studied the lightest Higgs boson mass in UU(1)′ models against various model parameters and particle masses. The model possesses a number of distinctive features not found in the MSSM: the presence of the heaviest Higgs boson H' (in addition to H and A present in the MSSM, all studied in detail in Fig. 3) as well as the μ_{eff} dependencies of the sfermion masses (studied in Figs. 1 and 2). Concerning LEP Higgs measurements, it is known that, bounds on the lightest Higgs boson in U(1)′ extensions are similar to that of the MSSM, but its upper bound is relaxed [11]. We have found rather generically that the LEP bounds constrain all four models we have considered. The Tevatron bounds, on the other hand, become effective for the X model, primarily. These are felt also by the ψ and N models (to a lesser extent than the X model); however, the η model yields fundamentally light h boson whose mass never nears the Tevatron forbidden band. Nevertheless, one concludes from the remaining three models that, the Tevatron bounds generically divide all model parameters in two disjoint ranges: those pertaining to low-mass domain and those to high-mass domain. For instance, the Higgsino Yukawa coupling h_s, as seen from Fig. 1, requires large (close to unity) values to elevate m_h above the Tevatron's upper limit i.e. ~ 168 GeV. This kind of restriction is seen also for other parameters, especially, the U(1)′ gauge coupling g'_Y (which needs to take large values close to $2g_Y$ to push m_h in the Tevatron territory in the models stemming from E(6) breaking).

In any case, at least for the parameter ranges considered, one achieves at the firm conclusion that the Tevatron bounds can rule out certain portions of the parameter space (as can be seen specially from Fig. 2). Of course, this is in accord with the case whether m_h is lying above or below the Tevatron exclusion limits. For instance, if $m_h \sim 168$ or higher then Higgsino Yukawa coupling should be larger than 0.6, for $m_h \sim 159$ or lower than this, Yukawa coupling of the singlet should be 0.5 or smaller according to our X model. Besides this we observe that, certain UU′ models such as the η model can be the first one to be ruled out since its m_h prediction is well below the Tevatron exclusion limits, even with a unrealistically enhanced (close to unity) gauge coupling g'_Y.

Concerning the stop masses, we found that X and E(6)-borrowed N, ψ models are highly sensitive to Tevatron (and any other collider bound) than in the MSSM due to the fact that μ_{eff} determines not only the LR (as in the MSSM) but also the LL and RR (unlike the MSSM) entries of the stop and sbottom mass-squared matrices. According to the model X, rule-outs of stop searches can help to determine whether the lightest Higgs boson is lying below or above the Tevatron Higgs mass measurements. Interestingly, low values of $m_{\tilde{t}_1}$ can help to narrow down the range of m_h. On the contrary, E(6)-based models can serve for the same aim, but with the opposite behavior. This is another important signature of the model-dependence surviving in UU(1)′ models.

Another interesting aspect observed within the models considered is that each model can predict a sensible splitting among m_A and m_H at varying order again in a model dependent fashion. In our examples, their masses are generally larger than 500 GeV, and hence, decoupled from the lightest Higgs (especially in X and N models). Additionally, their mass splittings can be as large as tens of GeVs in any model (much larger in η and ψ models). These observations also hold for splittings between Z' and H' masses.

The results found above, though unavoidably carry a degree of model dependence, can be directly tested at the LHC (and at the ILC with much higher precision). Measurements of the Higgs mass at the LHC, if turn out to prefer large values like 130–140 GeV or above, can be interpreted as preferring extensions of the MSSM like UU(1)′ models. Depending on the future exclusion limits, one might find more regions of parameter space excluded. For instance, if the Tevatron exclusion band widens down to 140 GeV border smaller and smaller values of h_s and $g_{Y'}$ become relevant. This limit also forces the remaining heavy Higgs bosons to decouple from the light spectrum. The plots presented in the figures are sufficiently ranged to cover possible developments in future exclusion limits (which may come form continuing analysis of the Tevatron data or from the early LHC data).

Acknowledgements

The works of D.D. and H.S. were partially supported by the Turkish Atomic Energy Agency (TAEK) via CERN-CMS Research Grant, and by the IYTE-BAP project.

References

[1] P. Langacker, arXiv:0901.0241 [hep-ph].
[2] J.E. Kim, H.P. Nilles, Phys. Lett. B 138 (1984) 150;
G.F. Giudice, A. Masiero, Phys. Lett. B 206 (1988) 480.
[3] M. Cvetič, D.A. Demir, J.R. Espinosa, L.L. Everett, P. Langacker, Phys. Rev. D 56 (1997) 2861, arXiv:hep-ph/9703317;
M. Cvetič, D.A. Demir, J.R. Espinosa, L.L. Everett, P. Langacker, Phys. Rev. D 58 (1998) 119905, Erratum;
P. Langacker, J. Wang, Phys. Rev. D 58 (1998) 115010, arXiv:hep-ph/9804428.
[4] D.A. Demir, G.L. Kane, T.T. Wang, Phys. Rev. D 72 (2005) 015012, arXiv:hep-ph/0503290;
A. Hayreter, Phys. Lett. B 649 (2007) 191, arXiv:hep-ph/0703269.
[5] S.M. Barr, Phys. Rev. Lett. 55 (1985) 2778;
J.L. Hewett, T.G. Rizzo, Phys. Rep. 183 (1989) 193;
M. Cvetič, P. Langacker, Phys. Rev. D 54 (1996) 3570, arXiv:hep-ph/9511378;
G. Cleaver, M. Cvetič, J.R. Espinosa, L.L. Everett, P. Langacker, Phys. Rev. D 57 (1998) 2701, arXiv:hep-ph/9705391;
G. Cleaver, M. Cvetič, J.R. Espinosa, L.L. Everett, P. Langacker, Nucl. Phys. B 525 (1998) 3, arXiv:hep-th/9711178;
D.M. Ghilencea, L.E. Ibanez, N. Irges, F. Quevedo, JHEP 0208 (2002) 016, arXiv:hep-ph/0205083.
[6] S.F. King, S. Moretti, R. Nevzorov, Phys. Rev. D 73 (2006) 035009, arXiv:hep-ph/0510419;
R. Diener, S. Godfrey, T.A.W. Martin, arXiv:0910.1334 [hep-ph].
[7] A. Ali, D.A. Demir, M. Frank, I. Turan, Phys. Rev. D 79 (2009) 095001, arXiv:0902.3826 [hep-ph].
[8] S.Y. Choi, H.E. Haber, J. Kalinowski, P.M. Zerwas, Nucl. Phys. B 778 (2007) 85, arXiv:hep-ph/0612218.
[9] M. Spira, P.M. Zerwas, Lect. Notes Phys. 512 (1998) 161, arXiv:hep-ph/9803257.
[10] D.A. Demir, L.L. Everett, Phys. Rev. D 69 (2004) 015008, arXiv:hep-ph/0306240.
[11] V. Barger, P. Langacker, H.S. Lee, G. Shaughnessy, Phys. Rev. D 73 (2006) 115010, arXiv:hep-ph/0603247.
[12] A. Hayreter, A. Sabanci, L. Solmaz, S. Solmaz, Phys. Rev. D 78 (2008) 055011, arXiv:0807.1096 [hep-ph].
[13] J.A. Casas, J.R. Espinosa, I. Hidalgo, JHEP 0411 (2004) 057, arXiv:hep-ph/0410298.

[14] R. Barate, et al., LEP Working Group for Higgs boson, Phys. Lett. B 565 (2003) 61, arXiv:hep-ex/0306033.
[15] T. Aaltonen, et al., CDF and D0 Collaborations, Phys. Rev. Lett. 104 (2010) 061802, arXiv:1001.4162 [hep-ex];
A. Dominguez, CDF and D0 Collaborations, AIP Conf. Proc. 1182 (2009) 138;
See the page: http://www-d0.fnal.gov/Run2Physics/WWW/results/prelim/HIGGS/H86/.
[16] D.A. Demir, L.L. Everett, P. Langacker, Phys. Rev. Lett. 100 (2008) 091804, arXiv:0712.1341 [hep-ph].
[17] D.A. Demir, L.L. Everett, M. Frank, L. Selbuz, I. Turan, arXiv:0906.3540 [hep-ph].
[18] P. Langacker, Rev. Mod. Phys. 81 (2008) 1199, arXiv:0801.1345 [hep-ph].
[19] J. Erler, P. Langacker, S. Munir, E.R. Pena, JHEP 0908 (2009) 017, arXiv:0906.2435 [hep-ph].
[20] See the page: http://www.phy.duke.edu/~kotwal/tifrDec08.pdf.
[21] V.M. Abazov, et al., D0 Collaboration, Phys. Rev. Lett. 101 (2008) 191801, arXiv:0804.3220 [hep-ex].
[22] C. Amsler, et al., Particle Data Group, Phys. Lett. B 667 (2008) 1.